

Laser Doppler vibrometry with acousto-optic frequency shift

PAWEŁ R. KACZMAREK, TOMASZ ROGOWSKI,
ARKADIUSZ J. ANTOŃCZAK, KRZYSZTOF M. ABRAMSKI

Institute of Telecommunications and Acoustics, Wrocław University of Technology,
Wybrzeże Wyspiańskiego 27, 50-370 Wrocław, Poland

This paper describes our experiments and investigations on vibration measurements by laser interferometers. The main objective was to build a simple heterodyne interferometer which would allow vibrations of objects with light scattering surface to be measured. The optimisation procedure of optical setup, basic heterodyne interferometer and results are presented.

Keywords: LDV, vibrometry, vibration measurements, heterodyne interferometry.

1. Introduction

It often appears necessary in practice to measure object vibrations. The more rigorous norms of sound noise emission require from designers and constructors of devices taking into account the negative influence of vibrations on environment. Usually, this is done by application of accelerometers or other mechanical methods. However, all commonly used methods have one basic disadvantage – the mechanical contact with vibrating object is the necessary condition. The influence of sensor in the case of measurement of large object vibrations is not substantial, but if the vibrating object has got a small mass (*e.g.*, a diaphragm of loudspeaker) such a sensor disturbs the value measured significantly. Besides, it is difficult to ensure the required physical contact between a transducer and a vibrating object in high temperatures and inaccessible places. Non-contact measuring methods utilising a coherent light (laser interferometry) have no such limitations. There are two main arrangements of the interferometric methods possible in vibration measurements: homodyne or heterodyne interferometry. The basic setup of Doppler shift measurement is the homodyne interferometer. This method is simple, but the necessity of determining the direction of movement makes the system much complicated. Measurement of movements or vibrations of the object that scatters light can be hard either. In practice, such a solution utilizes interference fringes counting method. This measurement is characterised by a small exactitude,

limited by resolution of the interference fringes (the use of additional signal processing allows the precision to be improved to 0.1 fringe) [1].

The main disadvantage of classical laser homodyne (single-frequency) interferometers applied in the laser vibrometry is the presence of intensity noise of laser radiation at low frequencies below 1 MHz. It causes that conversion of phase signal into intensity signal may produce a significant and harmful increase in the background noise levels. This problem may be overcome by the use of a heterodyne interferometer setup, where one of the beams is frequency shifted by passing it through frequency shifter (*e.g.*, acousto-optic Bragg modulator) [2] imposing frequency shift in the deflected beam. For the case of equal amplitudes of interfering beams in both arms of interferometer, the normalised signal from the photodetector is

$$s(t) = \left\{ 1 + \sin \left[2\pi \nu_B t + \phi(t) \right] \right\} \quad (1)$$

where $\phi(t)$ is the difference in phase of two arms and the ν_B is the frequency shift in, *e.g.*, Bragg modulator. This frequency should be well outside the $1/f$ noise region. As a result, a significant increase in the signal-to-noise ratio of over 20 dB is obtainable. When phase fluctuations $\phi(t)$ are periodic (stationary periodic vibrations), then they cause modulation of the intermediate frequency:

$$\nu_{IF} = \left\{ \nu_B + \frac{d\phi(t)}{dt} \right\}. \quad (2)$$

Standard phase modulation detection techniques may be used to extract the modulation. Stable offset frequency for heterodyne interferometry is required. It is quite easily obtainable by using Bragg modulator [3] with single or double Doppler shift ν_B , depending on the heterodyne setup. Typical Bragg frequency shifts are a few tens of MHz and flicker $1/f$ noise region is much lower than intermediate frequency.

2. Basic heterodyne interferometers

Our main target was to build a simple heterodyne interferometer which could be applied to measure vibrations of scattering light surfaces. The main criteria of choosing a proper setup were minimum number of optical elements needed and simple aligning of the setup.

A simple heterodyne interferometer with single frequency shift is shown in Fig. 1. In the arrangement presented laser beam crosses the Bragg cell and splits into two beams – zero and first-order ones [4]. The first of the beams falls on the measured object after passing the beamsplitter. Having been scattered on the surface the light is reflected from the beamsplitter and reaches a photodetector. The Bragg order beam after reflection in mirrors passes through the beamsplitter and interferes with the first beam on the photodetector. The FM modulated signal on the Bragg shift frequency ν_B

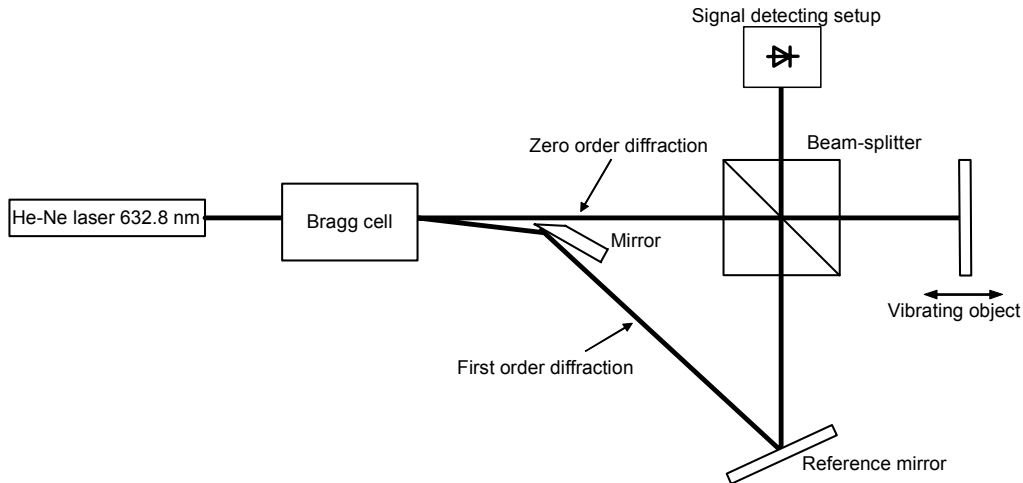


Fig. 1. Single Bragg shift configuration.

is received as a result of heterodyning. In this setup the separation between zero and first Bragg order beams is the main problem because of the small angle between beams. Additionally, the Bragg order beam (in this setup, reference one) is weakly modulated in amplitude due to deflection effect. As a result, the undesirable signal appears on a photodetector and masks the signal originated from vibrating object. To avoid this problem the frequency shift can be doubled by passing the beam twice through the Bragg modulator [5]. This arrangement is exceptionally simple (Fig. 2). The light beam crossing through the Bragg cell splits it into two, the zero order of diffraction – the reference beam (frequency ν_o) and the first order of diffraction – the measuring beam (frequency $\nu_o - \nu_B$). After reflection from the reference mirror and vibrating object respectively, beams are crossing through the Bragg cell again. The measuring beam falls on a photodetector (frequency changed by the Doppler phenomena $\nu_o - \nu_B \pm \nu_D$), whereas the reference beam deflects in the first order diffraction (frequency $\nu_o + \nu_B$).

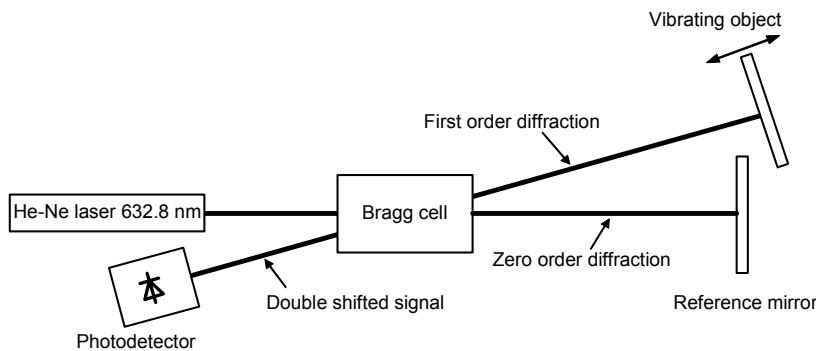


Fig. 2. Double Bragg shift configuration.

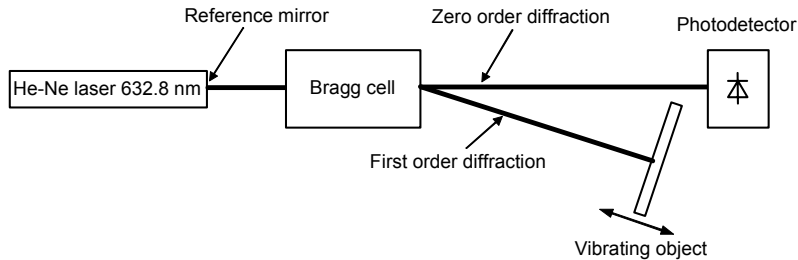


Fig. 3. Double Bragg shifted configuration with laser mirror.

The interference signal received on photodetector is $(\nu_o + \nu_B) - (\nu_o - \nu_B \pm \nu_D) = 2\nu_B \pm \nu_D$, and it forms the carrier at double Bragg frequency. Doppler-modulated signal gives information about the object's speed. In this case, disturbance caused by deflection effect does not influence signal from vibrating object. Unfortunately, the presence of even residual standing ultrasonic wave in the modulator causes undesirable amplitude modulation of beams on double Bragg frequency appearance – the same as the heterodyne signal. The next simplification of the setup can be made by means of a laser output mirror [6] – see Fig. 3. The reference beam passes through the Bragg modulator without frequency shift and the signal beam is deflected to the first order of diffraction (frequency $\nu_o + \nu_B$).

The beam scatters from the object and the frequency of the returning signal is $\nu_o + \nu_B \pm \nu_D$. After being Bragg shifted again the signal is reflected from the laser mirror and then passes through the Bragg modulator (without change of frequency) and gets on the photodetector, where it interferes with the reference beam. As a result of interference the received signal frequency is $(\nu_o + \nu_B \pm \nu_D + \nu_B) - \nu_o = 2\nu_B \pm \nu_D$ (the same as in the double Bragg shifted configuration). The disadvantages of this setup are quite similar to the previous one. Additionally, light coming back to the laser can disturb significantly its work conditions and cause a great increase in optical noise.

3. Undesirable effects

As a result of experiments with simple heterodyne interferometers we found two undesirable phenomena occurring in acousto-optic Bragg cells. The first one is a deflection effect, which is shown in Fig. 4. It appears in two cases: running and standing ultrasound wave. The light beam propagates in medium almost perpendicularly to the gradient of refraction index n and it deflects at the angle θ

$$\theta = L \text{grad}(n) \quad (3)$$

where L is the active length of Bragg cell. Beam deflection can cause intensity modulation at ultrasound frequency ν_B . In the case of the running ultrasound wave

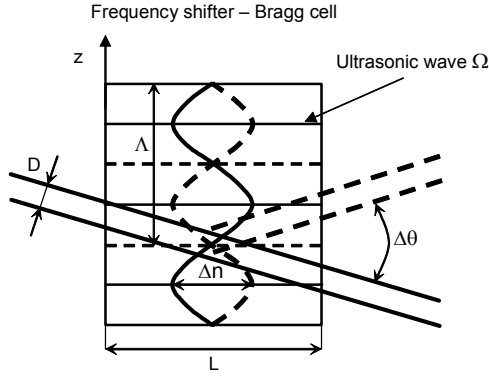


Fig. 4. Illustration of deflection effect.

propagating along the z axis the refraction index n is a sinusoidal variable,

$$n(t, z) = n_o + \Delta n \sin(Kz - \Omega t) \tag{4}$$

where: K – the ultrasound propagation coefficient, $\Omega = 2\pi \nu_B$ – the angular frequency of ultrasonic wave. In this case, $\text{grad}(n)$ is equal to:

$$\text{grad}(n) = \frac{2\pi\Delta n}{\Lambda} \cos(Kz - \Omega t) \tag{5}$$

where Λ is the ultrasound wavelength.

From Eqs. (3) and (5), change of deflection angle occurs with acoustic wave frequency Ω . Maximum angle of deflection is given by:

$$\Delta\theta_{\max} = 4\pi \frac{L}{\Lambda} \Delta n. \tag{6}$$

The effectiveness of the deflection depends on relation between ultrasonic wavelength and width of light beam. The gradient of refraction index is not constant across the beam diameter and the divergence of the laser beam occurs as a result of it [7]. The angle of divergence is

$$\delta\theta_c = \Delta\theta_{\max} - \Delta\theta|_{z=D/2+V_B t} = 4\pi \frac{L}{\Lambda} \Delta n \left(1 - \cos \frac{\pi D}{\Lambda} \right) \tag{7}$$

where D is a diameter of the light beam, V_B is a velocity of the ultrasound wave.

Different part of the beam reaches active surface of a photodetector in consequence. It causes the modulation of photocurrent frequency Ω . This effect can be reduced by

enlarging the light beam diameter, but this is unfavourable with regard to the limited size of the photodetector area and active area in the acoustooptic Bragg cell.

The second undesirable effect from the point of view of laser vibrometry is so-called standing wave effect. Bragg modulators can utilize standing or running ultrasonic wave. In the case of standing wave the intensity of the m -th order diffraction beam is proportional to a square of the m -th order Bessel function with an argument dependent on time

$$I_m = I_0 J_m^2(\Gamma_0 \cos(\Omega t)) \quad (8)$$

where Γ_0 is the coefficient dependent on intensity of ultrasonic wave and length of ultrasound interaction with the light. The intensity of light in zero diffraction order is:

$$I_0 = J_0^2(\Gamma_0 \cos(\Omega t)) \quad (9)$$

After spectral analysis of expression (9) one can obtain:

$$\begin{aligned} J_0^2(\Gamma_0 \cos(\Omega t)) = & \left[J_0^4\left(\frac{\Gamma_0}{2}\right) + 2 \sum_{a=1}^{\infty} J_a^2\left(\frac{\Gamma_0}{2}\right) \right] \\ & - \left[4 \sum_{a=0}^{\infty} J_a^2\left(\frac{\Gamma_0}{2}\right) J_{a+1}^2\left(\frac{\Gamma_0}{2}\right) \right] \cos(2\Omega t) \\ & + \left[2 J_1^4\left(\frac{\Gamma_0}{2}\right) + 4 \sum_{a=0}^{\infty} J_a^2\left(\frac{\Gamma_0}{2}\right) J_{a+2}^2\left(\frac{\Gamma_0}{2}\right) \right] \cos(4\Omega t) - \dots \end{aligned} \quad (10)$$

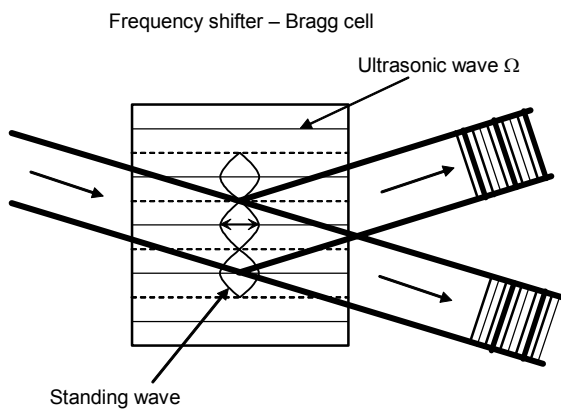


Fig. 5. Standing wave effect.

Expression (10) shows that the beam intensity in zero order diffraction is amplitude modulated frequency 2Ω and higher even harmonics. The occurrence of the intensity modulation in standing ultrasound wave appears because the time domain standing wave is equivalent to motionless phase grating with parameter Δn changing in time domain (Fig. 5). The depth of modulation in zero order depends on the value Γ_0 , however all non-zero diffraction orders are amplitude modulated with a hundred-percent efficiency and frequencies of that modulation are 2Ω , 4Ω , etc.

In the case of partial standing wave the observed effect is smaller (a decrease of modulation depth in all diffraction orders). The occurrence of even residual acoustic standing wave causes such undesirable intensity modulation of output beam. Hence, the spectral analysis of the second harmonic in the Bragg diffracted beam is a useful method for establishing usability of Bragg cells.

4. Configuration

After the analysis of the above configurations and effects which can disturb a heterodyne signal, important conclusions can be drawn about the principles of construction and optimisation of simple heterodyne interferometers:

- the reference beam which dominates in interference signal should not cross through the Bragg modulator to avoid its amplitude modulation;
- the very important matter is to prevent the light from returning to the laser and disturbing its work. This can be done by applying polarising optics.

As a result of the above analysis a practical model of heterodyne interferometer was developed (Fig. 6). The linearly polarised He-Ne laser was applied as a source of coherent light in the setup. The ratio between measurement and reference beams can be settled by changing polarization angle. The optimal value is 50:50. Light from the laser reaches polarisation beamsplitter to create two beams. The reference one after reflection from the mirror crosses beamsplitter and falls on the photodetector. The

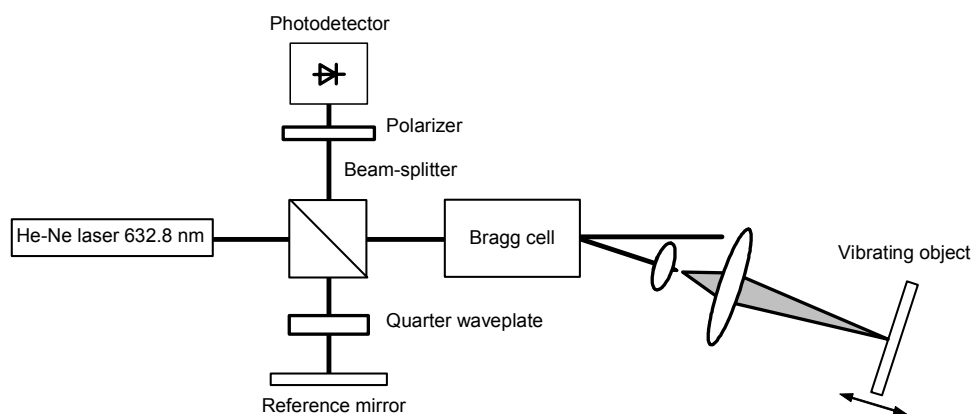


Fig. 6. Developed configuration.

quarter waveplate in connection with the mirror provides change of light polarization into orthogonal and ensures its passing through the beamsplitter instead of being reflected from it. The measuring beam passes through the Bragg cell (the frequency $\nu_o + \nu_B$), the set of lenses and then strikes incident the object. The set of lenses plays two roles – it increases the aperture of the setup and it focuses the beam on the object. For typical 3 meter measuring distance, the spot diameter on the object is about 100 μm . The light is scattered from the object surface and a small amount of it goes back to the system. Next, the light passes through the Bragg cell again (frequency $\nu_o + 2\nu_B \pm \nu_D$). The scattered light has not defined polarization which causes that it is not necessary to use the quarter waveplate in the arm of the interferometer. Its presence does not change the level of the heterodyne signal obtained from the setup. The additional advantage of this arrangement is that light reflected from lenses surface does not reach a photodetector and does not disturb measured signal. The utilization of the polarising optics causes reduction of optical power losses and the backcoupling to the laser is eliminated as well. As a photodetector sensitive p-i-n photodiode was applied. The signal level in this arrangement is about 20 dB higher than that on the arrangement from Fig. 2. The signal to noise ratio was over 20 dB for white sheet of xero paper as an object and measuring distance over 3 m. It was impossible to obtain such S/N ratio in other configurations.

The next step of our studies was to develop demodulation circuits. The signals coming from laser Doppler vibrometer have a wide spectrum. In the case of the model investigated in this work the frequency of signal is 160 MHz (double Bragg shift). This carrier wave is frequency modulated by the Doppler signal. The deviation of frequency depends linearly on the movement speed of measured object. In the case of using the He-Ne laser with wavelength $\lambda = 632.8$ nm the deviation is 1.58 MHz per 1 m/s of the velocity [8]. As a result, it is necessary to use FM demodulator which accepts a wide frequency spectrum. In the case of large amplitude of vibration the best choice is usage of a phase locked loop [9]. On the other hand, if sensitivity is a primary parameter – detection of very small vibrations – the demodulator should be a narrow-band one. For example, for the same laser and movement speed 1 $\mu\text{m/s}$ the Doppler frequency change is 1.58 Hz. The standard radio FM demodulator technique can fulfil proper and accurate demodulation. As is shown a large spread of signal frequencies coming from vibrometer requires at least two different demodulators to cover the whole measurement range.

5. Vibrometer calibration

To measure vibrations it is necessary to scale the electronics circuits. This can be done by using an object (standard) whose amplitude of vibrations is well known. It can be an exciter whose amplitude of vibrations is properly scaled thanks to measuring it in standard Michelson interferometer [10]. For scaling purposes, the exciter was driven with sinusoidal voltage and produced vibrations. Signals coming from the photodetector were observed at the oscilloscope. These signals were represented by

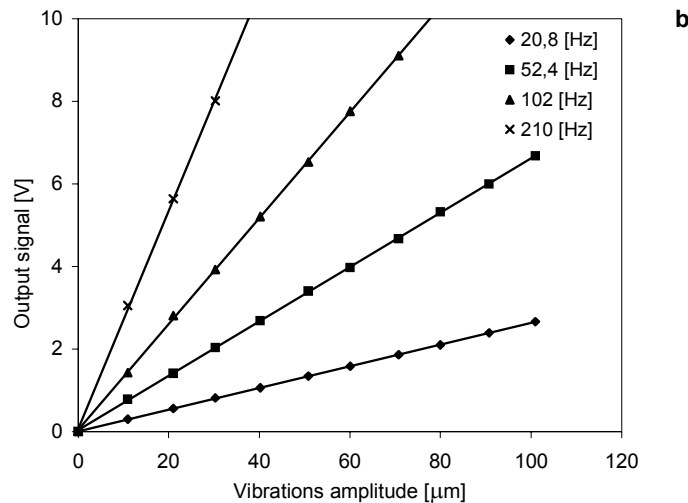
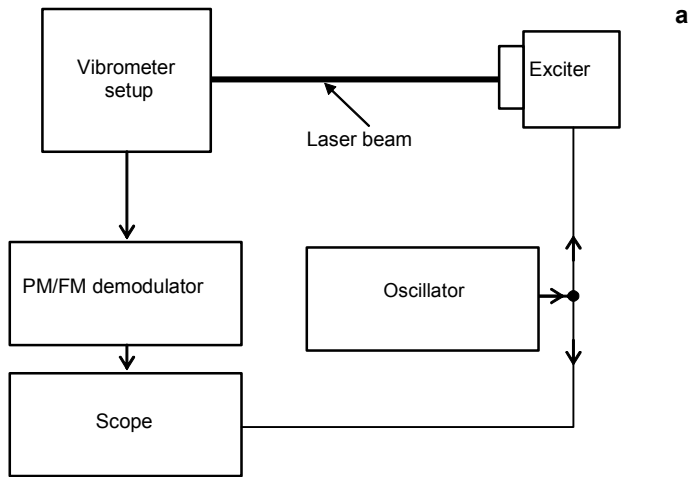


Fig. 7. Vibrometer calibration: **a** – setup, **b** – calibration data of the FM demodulator.

interference fringes as a result of optical length change in one of the arms in the interferometer. The amplitude of vibrations can be easily determined by counting the number of interference fringes occurring in half period of the vibrations. The voltage driving the exciter was used as a reference signal. After scaling of the exciter the next step was to calibrate the vibrometer (Fig. 7a). The exciter was driven by sinusoidal signals for which it had been scaled before. Assuming the linear dependence of vibration amplitude and value of the voltage driving the exciter it allowed us to make a scaling diagram (Fig. 7b) for different driving frequencies. The value of signal coming from vibrometer demodulator corresponds to the velocity of object. In the case of sinusoidal vibrations with settled frequency, the amplitude of vibrations is

proportional to the speed of movement. It permits calibration of the output signal from demodulator directly in the values of vibration amplitude. This method is inconvenient because of the necessity of graduation for every measured frequency and due to vibrations being limited exclusively to sinusoidal ones. To obtain calibration independent of the character of vibration and its frequency, the calibration procedure should rely on the velocity values because it is the natural signal from the Doppler vibrometer. This can be done for sinusoidal vibrations. The dependence between amplitude and velocity of vibrations in this case is given by the simple formula:

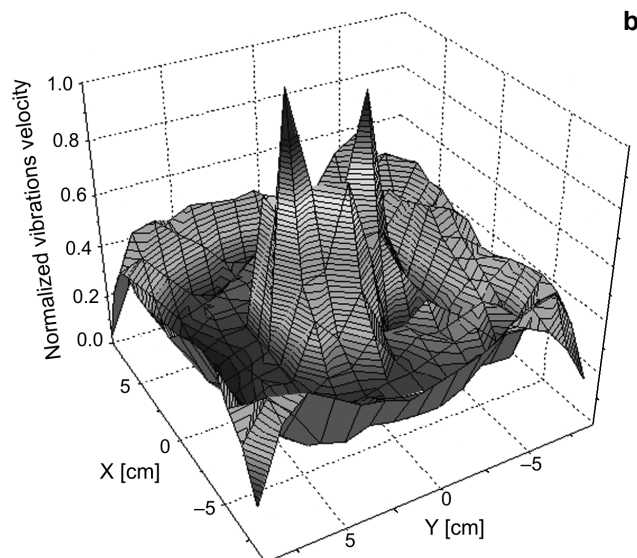
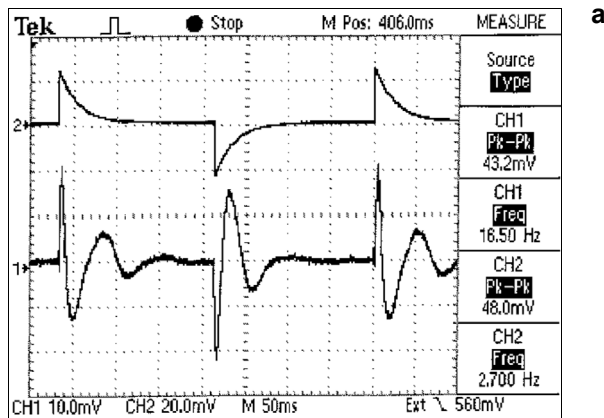


Fig. 8. Sample measurements made using the model of laser Doppler vibrometer: **a** – pulse response, **b** – two dimensional scan of loudspeaker's diaphragm.

$$V(t) = \omega A \cos(\omega t) \quad (11)$$

where $V(t)$ is the vibration velocity, A – the vibration amplitude, ω – the vibration angular frequency. Taking advantage of this one can determine sensitivity of vibrometer in velocity domain. For the setup described and the case of sinusoidal vibrations (Fig. 7b) it was 0.2 [V/(m/s)]. This value is correct for all types of vibrations, provided that spectrum of vibrations is contained in the frequency range of FM demodulator. To obtain amplitude signal from the vibrometer directly an integration of the output velocity signal (analogue or digital) should be applied.

6. Experimental results

Figure 8 shows some measurements performed by the vibrometer being constructed. Figure 8a demonstrates typical pulse response of a loudspeaker taken at the central point of the diaphragm. Trace 1 on the scope record is its velocity response and trace 2 is a driving signal of the loudspeaker. This vibration signal carries information about mechanical resonance frequency which can be determined by spectral analysis of that signal. Figure 8b presents two dimensional scan of vibrations of the loudspeaker's diaphragm at 1 kHz excitation. It is an example of mechanical modes analysis. It was performed by manual scanning from point to point. Measurement points were marked on the loudspeaker to provide satisfactory pointing accuracy about 1 mm with the raster size of 1 cm. In this case pointing precision is limited by hand-held accuracy, especially when the surface has a complex shape.

It should be considered that all measurements presented are scaled on velocity of the vibrating object (directly from FM demodulator without any integration circuits). Other parameters of vibrations can be obtained by mathematical analysis, the amplitude by integration of the velocity signal, the acceleration by derivation of the velocity signal. Measurements were performed with the use of an arrangement of demodulation based on PLL loop.

7. Conclusions

The main principles of how to build a simple and low cost heterodyne vibrometer have been shown. Two undesirable effects appearing in the Bragg modulator which are commonly utilized in the laser vibrometry have been presented. As has been shown the standing wave effect can be very a useful method for determining the Bragg cell applicability in this area. The workable model of the simple heterodyne interferometer which allows measurement of vibrations of objects with light scattering surface and the main principles of demodulation circuits design have been demonstrated. The calibrations of arrangement were presented as well. Some measurements of loudspeaker's diaphragm vibrations with application of designed vibrometer were performed.

Acknowledgments – This paper was inspired by V-th European Framework Program LAVINYA. The authors also acknowledge the support of the Foundation for Polish Science (FNP subsidies for scientists – 2001 edition, No. 1/2001).

References

- [1] GOPEL W., HESSE J., ZEMEL J.N., *Sensors. A Comprehensive Survey*, Vol. 6, VCH Publishers Inc., New York 1992.
- [2] JIANG CH., CHENG F., WU M., FENG Z., CHENG L., Proc. SPIE **2358** (1994), 93.
- [3] KORPEL A., *Acousto-optics*, Second Edition, Marcel Dekker, Inc., New York 1997.
- [4] SCOTT C.R., *Field Theory of Acousto-Optic Signal Processing Devices*, Artech House Inc., Norwood 1992.
- [5] CULSHAW B., *Optical Fibre Sensing and Signal Processing*, Peter Peregrinus Ltd., London 1984.
- [6] PETERSON R.W., ROBINSON G.M., CARLSEN R.A., ENGLUND C.D., MORAN P.J., WIRTH W.M., Appl. Opt. **23** (1984), 1464.
- [7] SALEH B.E.A., TEICH M.C., *Fundamentals of Photonics*, Wiley, New York 1991.
- [8] RINKEVICHUS B.S., Proc. SPIE **2729** (1996), 62.
- [9] KEESE W.O., *An Analysis and Performance Evaluation of and Passive Filter Design Technique Handicap Charge Pump Phase – Locked Loops*, National Semiconductor, Application Note 1001, May 1996.
- [10] ABRAMSKI K.M., KACZMAREK P.R., ROGOWSKI T.J., ANTONCZAK A.J., Proc. SPIE **4072** (2000), 37.

*Received November 21, 2003
in revised form April 16, 2004*